The Thermochemistry of Phosphorus Tetrahalide Anions†

Terry E. Heil, Catherine E. Check, Kim C. Lobring, and Lee S. Sunderlin*

Department of Chemistry and Biochemistry, Northern Illinois University, DeKalb, Illinois 60115

Received: June 11, 2002; In Final Form: July 22, 2002

The Br_3P-Br^- and I_3P-I^- bond strengths have been determined by measuring thresholds for collision-induced dissociation in a flowing afterglow-tandem mass spectrometer. The results are combined with previously determined values for the PF_4^- and PCl_4^- systems to determine the effect of the terminal atom on hypervalent bond strengths. The bond strengths correlate very well with the difference in the electronegativities of phosphorus and the halogen atoms. Computational results at the B3LYP/6-311+G(d) level indicate that PCl_4^- and PBr_4^- have seesaw geometries and are good examples of three-center, four-electron bonding. PF_4^- has a similar geometry, but the bonding is more ionic, whereas PI_4^- is tetrahedral, consistent with greater steric crowding.

Introduction

Group 15 trihalide molecules AX_3 (A = P, As, Sb, and Bi and X = F, Cl, Br, and I) obey the octet rule. Nevertheless, they act as electron-pair acceptors to form the corresponding tetrahalide anions AX_4^-. Although phosphorus trihalides are weaker Lewis acids than the corresponding arsenic, antimony, and bismuth systems, both in solution[1] and in the gas phase,[2] PF_4^-,[3] PCl_4^-,[4] and PBr_4^- [5−7] have been reported in condensed phases. These anions are examples of hypervalent bonding[8−10] because their Lewis structures show 10 electrons around the central atom. Experiments on these ions in the gas phase allow hypervalent bonding to be studied in the absence of solvent or lattice effects.[11]

Larson and McMahon[12] previously reported $D(F_3P-F^-)$ = 168 kJ mol^{-1}. This value, which comes from a fluoride affinity scale based on a series of measurements of relative bond energies, should be adjusted to ca. 200 kJ mol^{-1} because of changes in the affinity scale.[13−15] Recently, our group has measured $D(Cl_3P-Cl^-)$ = 90 ± 7 kJ mol^{-1}.[2] This paper discusses gas-phase measurements of the PBr_3-Br^- and PI_3-I^- bond strengths. These can be combined with the data mentioned above to give a complete set of PX_3-X^- bond strengths to determine the effects of the *terminal* atom on hypervalent bond strengths in these systems. The results provide a comparison to recent results on the ACl_4^- systems,[2] which explore the effect of changing the *central* atom on the bond strength.

Three main models have been used to explain how hypervalent bonding occurs. The expansion of the octet through the use of d orbitals is now generally viewed as unimportant,[16,17] although introductory textbooks still use this model.[18] The three-center four-electron (3C-4E) model,[8,19−22] where three p orbitals aligned with a molecular axis are used to form three molecular orbitals, is now more commonly accepted. This model is illustrated in Figure 1. The third model emphasizes the importance of ionic bonding in hypervalent systems.[23,24] The 3C-4E model is implicitly partially ionic, with charges of −0.5 on each of the terminal atoms. This "semi-ionic"[3] nature is emphasized in the Lewis description of a hypervalent XAX^- system as a resonance hybrid: $X-A:X^- \Leftrightarrow X^-:A-X$.[25] The data from this work are compared to these models below.

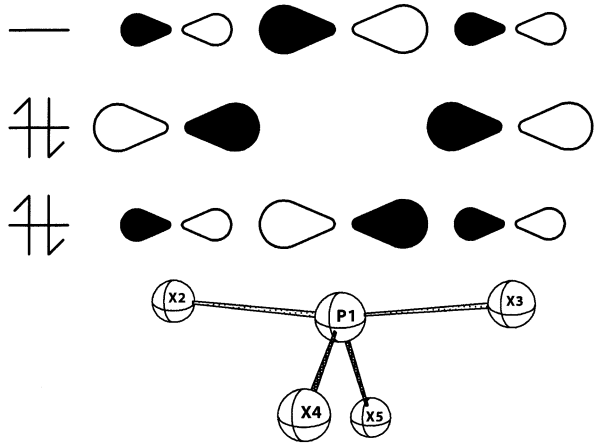

Figure 1. Bonding in the seesaw geometry for AX_4^- systems. Atoms 2 and 3 are termed axial, and atoms 4 and 5 are termed equatorial.

It is generally difficult to compute bond strengths in hypervalent compounds because of strong electron correlation effects.[26−28] The majority of the computational studies on group 15 halides have focused on bond energies and electron affinities for phosphorus fluorides[28−31] and phosphorus chlorides.[32] Computational work on PBr_4^- and PI_4^- is lacking; moderately high level calculations on these systems are also described below.

Experimental Section

Bond strengths were measured using the energy-resolved collision-induced dissociation (CID) technique[33,34] in a flowing afterglow-tandem mass spectrometer (MS).[35] The instrument consists of an ion source region, a flow tube, and the tandem MS. The dc discharge ion source used in these experiments is typically set at 2000 V with 2 mA of emission current. The flow tube is a 92 cm × 7.3 cm i.d. stainless steel pipe that operates at a buffer gas pressure of 0.4 Torr, a flow rate of 200 standard cm^3 s^{-1}, and an ion residence time of 10 ms. The

† Part of the special issue "Jack Beauchamp Festschrift".

* Corresponding author. E-mail: sunder@niu.edu. Phone: 815-753-6870. Fax: 815-753-4802.

10.1021/jp021386y CCC: $22.00
Published on Web 08/30/2002

buffer gas is helium with up to 10% argon added to stabilize the dc discharge.

To make PBr_4^- for this study, PBr_3 was added to the ion source. Electron impact on PBr_3 produces Br^-, which adds to PBr_3 to form PBr_4^-. Approximately 10^5 collisions with the buffer gas cool the metastable ions to room temperature. For PI_4^-, PI_3 (which has a lower vapor pressure) was heated in a round-bottom flask that was grooved and wrapped with coils of Nichrome heating wire. I_2 was also added to create additional I^-.

The tandem MS includes a quadrupole mass filter, an octopole ion guide, a second quadrupole mass filter, and a detector, contained in a stainless steel box that is partitioned into five interior chambers. Differential pumping on the five chambers ensures that further collisions of the ions with the buffer gas are unlikely after ion extraction. During CID experiments, the ions are extracted from the flow tube and focused into the first quadrupole for mass selection. The reactant ions are then focused into the octopole, which passes through a reaction cell that contains Xe collision gas (the previous work on PCl_4^-, a lighter ion, used Ar as the collision gas). After the dissociated and unreacted ions pass through the reaction cell, the second quadrupole is used for mass analysis. The detector is an electron multiplier operating in pulse-counting mode.

The energy threshold for CID is determined by modeling the cross section for product formation as a function of the reactant ion kinetic energy in the center-of-mass (CM) frame, E_{cm}. The octopole is used as a retarding field analyzer to measure the reactant ion beam energy zero.[34] The ion kinetic energy distribution is typically Gaussian with a full-width at half-maximum of 1.2 eV (1 eV = 96.5 kJ mol^{-1}). The octopole offset voltage measured with respect to the center of the Gaussian fit gives the laboratory kinetic energy, E_{lab}, in electronvolts. Low offset energies are corrected for truncation of the ion beam.[36] To convert to the center-of-mass (CM) frame, the equation $E_{cm} = E_{lab}m(m + M)^{-1}$ is used, where m and M are the masses of the neutral and ionic reactants, respectively. All experiments were performed with both mass filters at low resolution to improve ion collection efficiency and reduce mass discrimination. Average masses were used for Br and Xe, which have substantial populations of two or more isotopes.

The total cross section for a reaction, σ_{total}, is calculated using eq 1, where I is the intensity of the reactant ion beam, I_o is the intensity of the incoming beam ($I_o = I + \sum I_i$), I_i is the intensity of each product ion, n is the number density of the collision gas, and l is the effective collision length, 13 ± 2 cm. Individual product cross sections σ_i are equal to $\sigma_{total}(I_i/\sum I_i)$.

$$I = I_o \exp(-\sigma_{total} nl) \quad (1)$$

Threshold energies are derived by fitting the data to a model function given in eq 2, where $\sigma(E)$ is the cross section for formation of the product ion at center-of-mass energy E, E_T is the desired threshold energy, σ_o is the scaling factor, n is an adjustable parameter, and i denotes rovibrational states having energy E_i and population g_i ($\sum g_i = 1$). Doppler broadening and the kinetic energy distribution of the reactant ion are also accounted for in the data analysis, which is done using the CRUNCH program written by Armentrout and co-workers.[34,36]

$$\sigma(E) = \sigma_o \sum_i g_i (E + E_i - E_T)^n / E \quad (2)$$

Although the PX_3 vibrational frequencies[37] and some of the PX_4^- vibrational frequencies[3,5,38] are known, the available data are not complete, and condensed-phase intermolecular interactions may affect the available data. Therefore, vibrational and rotational frequencies were calculated using the B3LYP method and the 6-311+G(d) basis set. For iodine, the 6-311G(d) basis set[39] was supplemented with a diffuse (+) function taken from another iodine basis set.[40] The frequencies are given in Table 1. The calculated frequencies are lower than the known experimental values by an average of 5%, a typical result for this type of system.[2] Uncertainties in the derived thresholds due to possible inaccuracies in the frequencies were estimated by multiplying the entire sets of frequencies by 0.9 and 1.1. The resulting changes in internal energies were less than 1 kJ mol^{-1}. Therefore, the calculated frequencies were used without scaling. Polarizabilities for PX_3 products were also taken from the computational results; varying the calculated values by 50% had a negligible effect on the derived thresholds.

TABLE 1: Calculated Rotational and Vibrational Constants for PBr_4^- and PI_4^- [a]

	X = Br exp	X = Br calc	X = I exp	X = I calc
PX_3 vib	113 (×2)	105 (×2)	79 (×2)	71.0 (×2)
	160	152	111	107
	384 (×2)	369 (×2)	325 (×2)	315 (×2)
	390	372	303	295
PX_3 rot		0.0171		0.0084
		0.0323 (×2)		0.0163 (×2)
PX_4^- vib		42.1		22.5 (×3)
		61.2		
		76.6		
		84.7		34.0 (×2)
		107		
		136		121
		228		246 (×3)
		339		
		346		
PX_4^- rot		0.0108		0.0067 (×3)
		0.0123		
		0.0206		

[a] Values in cm^{-1}. Experimental values from ref 37. Calculated values obtained using B3LYP/6-311+G(d).

Collisionally activated metastable complexes can have sufficiently long lifetimes that they do not dissociate on the experimental time scale (ca. 150 μs). Such kinetic shifts are accounted for in the CRUNCH program by RRKM lifetime calculations.[34] The relatively small molecules studied in this work have small kinetic shifts, less than 0.2 kJ mol^{-1}. The uncertainty in the derived thresholds is again estimated by multiplying reactant or product frequency sets by 0.9 and 1.1, and by multiplying the time window for dissociation by 10 and 0.1. The effect of these variations is less than 1 kJ mol^{-1}.

An ion not sufficiently energized by one collision with the target gas may gain enough energy in a second collision to be above the dissociation threshold. This effect is eliminated by linear extrapolation of the data taken at several pressures to a zero pressure cross section before fitting the data.[41]

Computational work on these systems was performed using the Gaussian 98 Suite.[42] The Natural Bond Order Analysis (NBO 5.0)[43] and Atoms In Molecules (AIM)[44−46] programs were also used to study the nature of the bonding in these systems. The AIM bond order calculation for PBr_4^- did not converge using the B3LYP/6-311+G(d) method, so a value calculated using the 3-21G(d) basis set augmented by a diffuse function[40] was used; previous calculations suggest that the results are not very dependent on basis set.[2]

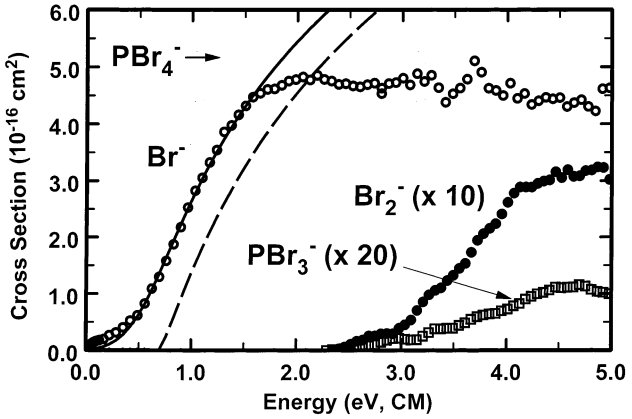

Figure 2. Cross section for collision-induced dissociation of PBr_4^- as a function of energy in the center-of-mass frame. The solid and dashed lines represent convoluted and unconvoluted fits to the data, as discussed in the text.

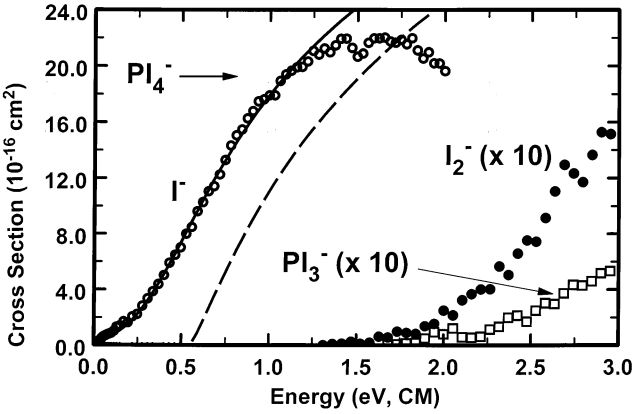

Figure 3. Cross section for collision-induced dissociation of PI_4^- as a function of energy in the center-of-mass frame. The solid and dashed lines represent convoluted and unconvoluted fits to the data, as discussed in the text.

TABLE 2: Fitting Parameters for CID of PX_4^- Anions[a]

X	E_T (eV)	n
Cl[b]	0.93 ± 0.06	1.23 ± 0.05
Br	0.68 ± 0.06	1.34 ± 0.13
I	0.57 ± 0.08	1.32 ± 0.15

[a] See text for discussion of fitting parameters. [b] Reference 2.

Results

CID of PX_4^- (X = Br and I) gives reaction 3, loss of X^-, as the predominant product. Reactions 4 and 5, formation of PX_3^- and X_2^-, are observed as minor products at higher energies. Appearance curves for CID of these anions are shown in Figures 2 and 3.

$$PX_4^- \rightarrow PX_3 + X^- \quad (3)$$

$$PX_4^- \rightarrow PX_3^- + X \quad (4)$$

$$PX_4^- \rightarrow PX_2^- + X_2 \quad (5)$$

The eq 2 fitting parameters are given in Table 2, and the fits are shown in Figures 2 and 3 as well. The cross sections for minor products are negligible in the threshold region and are not included in the fit. Because the effects of reactant and product internal energy are included in the fitting procedure, the dissociation thresholds correspond to bond energies at 0 K.

TABLE 3: Bond Dissociation Enthalpies for PX_4^- Anions[a]

X	0 K	298 K	theo (0 K)[b]	theo (0 K)[c]
F	200 ± 10	200 ± 10[d]	210	197
Cl	90 ± 7[e]	90 ± 7[e]	107	103
Br	66 ± 6	65 ± 6	98	93
I	55 ± 8	54 ± 8	102	

[a] Values in kJ mol^{-1}. [b] Calculated using B3LYP/6-311+G(d) (see text for basis set details). [c] Calculated using G2(MP2). [d] Reference 12, adjusted as discussed in the text. [e] Reference 2.

TABLE 4: Structural Properties of PX_4^- and PX_3[a]

	PX_4^-				PX_3	
X	R_{12}	R_{14}	$\angle_{213}$	$\angle_{415}$	R_{PX}	$\angle_{XPX}$
F	180	165	188.6	87.2	161	97.5
Cl	246	213	168.2	93.7	209	101.0
Br	263	232	158.1	96.9	227	102.2
I	272	272	109.5	109.4	252	103.9

[a] Bond distances in picometers and angles in degrees calculated using B3LYP/6-311+G(d). For atom labels refer to Figure 1.

TABLE 5: Calculated Atomic Charges[a]

		PX_4^-			PX_3	
technique	X	q_P	q_X(ax)	q_X(eq)	q_P	q_X
AIM	F	2.07	−0.77	−0.76	2.21	−0.74
	Cl	1.10	−0.062	−0.43	1.17	−0.39
	Br	0.83	−0.58	−0.34	0.79	−0.26
	I	0.47	−0.37	−0.37	0.31	−0.10
NBO	F	1.52	−0.66	−0.60	1.68	−0.56
	Cl	0.79	−0.58	−0.32	0.76	−0.25
	Br	0.52	−0.51	−0.25	0.51	−0.17
	I	0.06	−0.27	−0.27	0.10	−0.03

[a] Calculated at the B3LYP/6-311+G(d) level.

TABLE 6: AIM Bond Orders[a]

X	BO(PX_4^-,ax)	BO(PX_4^-,eq)	B(PX_3)	ax/PX_3	eq/PX_3
F	0.63	0.64	0.73	0.86	0.88
Cl	0.75	1.03	1.09	0.69	0.95
Br	0.82	1.10	1.18	0.69	0.93
I	1.06	1.06	1.24	0.86	0.86

[a] Calculated at the 6-311+G(d) level except as noted in the Experimental Section.

The final uncertainties in the bond energies are derived from the standard deviation of the thresholds determined for individual data sets, the uncertainty in the reactant internal energy, the effects of kinetic shifts, and the energy scale uncertainty (±0.15 eV lab). The results are given in Table 3.

Computed bond energies, structures, atomic charges, and bond orders are given in Tables 4−6. The 0 K bond energies can be converted into 298 K bond enthalpies (Table 3) using the heat capacities of the reactants and products, which can be determined using the frequencies from Table 1. The reactant and product heat capacities are very similar, so the 298 K bond enthalpies are almost identical to the 0 K values.

Discussion

Calculated Geometries, Atomic Charges, and Bond Orders. The 3C-4E model predicts that equatorial bonds in PX_4^- should be two-center, two-electron bonds similar to those in PX_3, whereas the axial (3C-4E) bonds should be longer. If the bonding is ionic, all four bonds should be of similar length. Computed bond lengths and angles are given in Table 4. For X = Cl and Br, R_{12} in PX_4^- is only 4−5 pm longer than R_{PX} in PX_3, whereas R_{14} is 36−37 pm longer. Although the experi-

mental crystal structures for PCl_4^- and PBr_4^- are distorted by lattice effects,[4,6,7] the average axial and equatorial bond lengths are consistent with the computational results. The substantial difference in bond lengths agrees with the 3C-4E model. The difference between the axial and equatorial bond lengths in PF_4^- (15 pm) is less than half as large as that in PCl_4^- and PBr_4^-, consistent with increased ionic character in PF_4^-. Surprisingly, the differences between the respective axial and equatorial bond lengths in PF_5 and PCl_5 (4 and 12 pm)[47] are much smaller than the corresponding values for PX_4^-.

The calculations give a tetrahedral geometry for PI_4^- rather than a seesaw. This can be understood in terms of two limiting geometries for PX_4^- systems. If the lone pair on the P atom is stereochemically active, five active electron pairs around the central atom lead to a seesaw geometry. If the lone pair is stereochemically inactive, then the four active electron pairs lead to a tetrahedral geometry. As noted by Cotton et al.,[48] "Stereochemical activity of the lone pair decreases with (1) increasing coordination numbers, (2) increasing atomic number of the halogen, and especially (3) increasing atomic number of [the central element]."[49] Sheldrick et al. found that PBr_4^- is partially distorted toward a tetrahedral geometry.[6] The greater steric repulsion of heavier halogen ligands[1] is also seen in the computational results, where $\angle_{213}$ decreases by 30° and $\angle_{415}$ increases by 10° in going from PF_4^- to PBr_4^-. The calculations indicate that PI_4^- continues this trend. An example of the third effect is $BiCl_4^-$, which is calculated to be nearly tetrahedral.[2] Thus, competing forces in AX_4^- molecules favor two different geometries.

The 3C-4E model predicts charges of −0.5 for the axial halides and 0 for the other atoms in PX_4^-. The calculated atomic charges for PCl_4^- and PBr_4^- given in Table 5 are only partially consistent; the differences in the equatorial and axial charges for PCl_4^- and PBr_4^- range from 0.19 to 0.26, and the charges in PF_4^- are nearly the same. P−X bond polarity appears to be an important effect on the atomic charges; the fluoride species in particular is calculated to be more ionic than covalent. The AIM and NBO calculations agree that addition of X^- to PX_3 causes only minor changes in the charge on the central atom. Calculated NBO charges on the axial and equatorial halogen atoms in PF_5 and PCl_5 are different by only 0.04 and 0.12, respectively. This, like the bond lengths given above, suggests that the axial and equatorial halogens in PX_5 are more similar than the corresponding halogens in PX_4^-.

The best interpretation of the AIM bond orders given in Table 6 is not obvious because the nominal single bonds in ACl_3 have calculated bond orders ranging from 0.73 to 1.24, with lower bond orders correlating with more ionic bonding. However, the *ratios* of the bond orders in PX_4^- to the bond orders in PX_3 give clearer trends. According to the 3C-4E model, the equatorial (two-center, two electron) P−X bonds should have a bond order of 1, whereas the axial bonds should be 3C-4E bonds with P−X bond orders of ca. $2^{-0.5}$ (0.71).[50] If ionic bonding is dominant, the four P−X bonds in PX_4^- should have similar bond orders. Given this simplified description, the relative bond orders (also given in Table 6) have clear implications: PCl_4^- and PBr_4^- are in good agreement with the 3C-4E model. PF_4^-, which has four similar bond orders, is ionic. PI_4^- has four identical bond orders, which are similar to bond orders in PF_4^-. However, the cause is the tetrahedral geometry rather than the difference in the electronegativities of the phosphorus and the halogen.

NBO (Natural Population Analysis) calculations show 3C-4E bonding in PF_4^-, PCl_4^-, and PBr_4^-, but not in PI_4^-. This is consistent with the two different geometries discussed above.

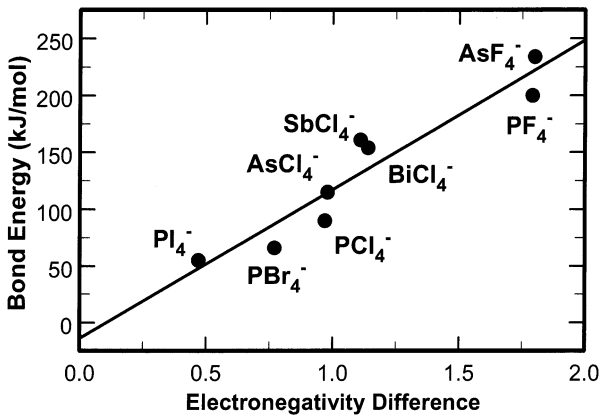

Figure 4. Bond energies in AX_4^- systems as a function of the difference in Pauling electronegativity between the central atom and the halogen atom. Data from the present work and refs 12 and 15.

The NBO calculations also give total valence d orbital occupancies of 0.02−0.06 electrons in all PX_3 and PX_4^- systems, with the PX_3 systems having higher d orbital occupancies than the PX_4^- systems. This supports the idea that d orbitals on the central atom do not participate significantly in the bonding molecular orbitals of the molecule; a similar effect was seen for the other ACl_4^- molecules.[2]

Trends in Bond Strengths. As shown in Table 3, the X_3P-X^- bond strength is strikingly weaker for X = Cl than for X = F. The X = Br and I values continue the downward trend. A parallel trend is seen in the two available X_3As-X^- bond strengths. $D(F_3As-F^-)$ has been previously measured to be 34 kJ mol^{-1} higher than $D(F_3P-F^-)$.[12] $D(Cl_3As-Cl^-) = 115 \pm 7$ kJ mol^{-1}, 25 kJ mol^{-1} higher than $D(Cl_3P-Cl^-)$.[2]

Part of the observed trend can be attributed to a general weakening of P−X bonding for X lower on the periodic table. For example, the average of the 298 K bond enthalpies in PX_3, $D(P-3X)/3$, are 504, 323, 266, and 200 kJ mol^{-1} for X = F, Cl, Br, and I, respectively.[51]

The eight AX_4^- bond strengths currently known can be plotted as a function of the difference in electronegativity between the terminal and central atoms (ΔEN). The results are shown in Figure 4. Clearly, the AX_3-X^- bond energies correlate well with ΔEN ($R^2 = 0.92$). There are several factors that potentially contribute to this effect, and the bond strengths in PX_3 given above indicate that much of the effect is due to factors that are not unique to 3C-4E bonding.

Arguably, the data for PI_4^- should not be included in Figure 4 because the geometry and bonding are not the same as in the other species. However, the seesaw geometry is apparently at nearly the same energy as the tetrahedral structure. Calculations at the B3LYP/6-311+G(d) level indicate that if the geometry of PI_4^- is constrained such that $\angle_{213} = 158.1°$ (the value in PBr_4^-), the energy is only 9 kJ/mol higher than the value at the fully optimized geometry. Thus, the bond energy in the seesaw geometry is apparently slightly weaker than the measured bond energy, and the difference does not significantly affect the results in Figure 4.

The data in Figure 4 represent systems where ΔEN is small (and the 3C-4E model is apparently better) as well as systems where ΔEN is almost 2 (and the ionic description is more consistent with the computational results). Nevertheless, the linear regression shown in Figure 4 shows no discontinuity, suggesting a continuum of bonding between the two limits described by the two models. The slope of the fit, 140 kJ mol^{-1}

per electronegativity unit, is inconsistent with the expanded octet model, which does not involve charge buildup on the terminal atoms.

Larson and McMahon[12] measured $D(F_3P-Cl^-) = 65$ kJ mol^{-1} and $D(F_3As-Cl^-) = 108$ kJ mol^{-1}. These are slightly weaker than the corresponding $D(Cl_3A-Cl^-)$ values given above. If the bonding were dominated by an ion−dipole attraction between the Cl^- and the polar AX_3 molecule, then the ability of F to withdraw more electron density from A should make $D(F_3A-Cl^-)$ *stronger* than $D(Cl_3A-Cl^-)$. Thus, ion−dipole interactions do not dominate the bond strengths.

The calculated bond strengths in Table 3 are reasonably good for the fluoride and chloride systems but diverge for the bromide and iodide systems. This is surprising, because calculations on the closely related trihalide systems are generally worse for the lighter halogens.[26] The B3LYP calculations give higher bond strengths than the more computationally intensive G2(MP2) calculations, which is consistent with results for similar systems.[52]

The current data suggest that bond strengths in other hypervalent systems may be predicted with reasonable accuracy if the electronegativities of the atoms involved are known. However, interpolation of the data suggests that NF_4^- is bound by ca. 100 kJ mol^{-1}, whereas the experimental value is 30 kJ mol^{-1}.[53] Similarly, the bond strength in F_3^- is about 30 kJ mol^{-1} weaker than the bond strengths in Br_3^- and I_3^-, even though $\Delta EN = 0$ for these systems.[54] A theoretical calculation at the B3LYP/aug-cc-pVDZ level gives $D(NF_3-F^-) = 54$ kJ mol^{-1}; calculations at this level give a similar overestimate of the bond strength in F_3^-.[54] The deviation of the experimental bond strengths from the typical trend may be due to the lack of d orbitals on the central atom in NF_4^- and F_3^-, eliminating the possibility of π-back-bonding from filled lone pairs on the halogen atoms;[55] differences between the orbitals of σ symmetry on the central atom may also play a role.[56]

Work in progress on trihalide systems shows a similar dependence of bond strength on ΔEN, but with a substantially higher *y*-intercept. The cause of the difference in the intercepts is not clear; further work will explore these bond strength trends in more detail.

Conclusions

The Br_3P-Br^- and I_3P-I^- bond strengths at 0 K have been determined to be 66 ± 6 and 55 ± 8 kJ mol^{-1} by measuring thresholds for collision-induced dissociation in a flowing afterglow-tandem mass spectrometer. The bond strengths for all four phosphorus tetrahalide anions correlate very well with the difference in the electronegativities of phosphorus and the halogen atoms; the slope of 140 kJ mol^{-1} per electronegativity unit indicates the importance of this effect. Computational results at the B3LYP/6-311+G(d) level suggest that PCl_4^- and PBr_4^- have near-linear, three-center, four-electron bonds, whereas PF_4^- is more ionic. Steric crowding makes 3C-4E bonding energetically unfeasible in PI_4^-, which is tetrahedral instead. The calculated bond strengths for PBr_4^- and PI_4^- are substantially higher than the experimental bond energies; the cause for this is not known.

Acknowledgment. This work was funded by the National Science Foundation, grant CHE-9985883. We thank Peter Armentrout, Kent Ervin, and Mary Rodgers for use of the CRUNCH software for data analysis, Thomas Gilbert for assistance with the computational work, and the NIU Computational Chemistry Laboratory for computer time.

References and Notes

(1) Wiberg, N. *Holleman-Wiberg Inorganic Chemistry*, 1st English ed.; Academic Press: San Diego, 2001.

(2) Walker, B. W.; Check, C. E.; Lobring, K. C.; Pommerening, C. A.; Sunderlin, L. S. *J. Am. Soc. Mass Spectrom.* **2002**, *13*, 469−476.

(3) Christe, K. O.; Dixon, D. A.; Mercier, H. P. A.; Sanders, J. C. P.; Schrobilgen, G. J.; Wilson, W. W. *J. Am. Chem. Soc.* **1994**, *116*, 2850−2858.

(4) Dillon, v. K. B.; Platt, A. W. G.; Schmidpeter, A,; Zwaschka, F.; Sheldrick, W. S. *Z. Anorg. Allg. Chem.* **1982**, *488*, 7−26.

(5) Dillon, K. B.; Waddington, T. C. *J. Chem. Soc., Chem. Commun.* **1969**, 1317.

(6) Sheldrick, W. S.; Schmidpeter, A.; Zwaschka, F.; Dillon, K. B.; Platt, A. W. G.; Waddington, T. C. *J. Chem. Soc., Dalton Trans.* **1981**, 413−418.

(7) Scheldrick, W. S.; Kiefer, J. *Z. Naturforsch. B* **1989**, *44*, 609−611.

(8) Reed, A. E.; Schleyer, P. v. R. *J. Am. Chem. Soc.* **1990**, *112*, 1434−1445.

(9) Norman, N. C. *Periodicity and the P-block Elements*; Oxford University Press: Oxford, U.K., 1994.

(10) Magnusson, E. *J. Am. Chem. Soc.* **1990**, *112*, 7940−7951.

(11) Sunderlin, L. S. Hypervalent Bonding in Gas-Phase Anions. In *Advances in Gas-Phase Ion Chemistry*; Adams, N., Babcock, L., Eds.; JAI Press: Greenwich, CT, 2001; Vol. 4.

(12) Larson, J. W.; McMahon, T. B. *J. Am. Chem. Soc.* **1983**, *105*, 2944−2950. Larson, J. W.; McMahon, T. B. *J. Am. Chem. Soc.* **1985**, *107*, 766−773.

(13) Bogdanov, B.; Peschke, M.; Tonner, D. S.; Szulejko, J. E.; McMahon, T. B. *Int. J. Mass Spectrom.* **1999**, *185*, 707−725.

(14) Wenthold, P. G.; Squires, R. R. *J. Phys. Chem.* **1995**, *99*, 2002−2005.

(15) Lobring, K. C.; Check, C. E.; Sunderlin, L. S. *Int. J. Mass Spectrom.*, in press.

(16) Heard, G. L.; Marsden, C. J.; Scuseria, G. E. *J. Phys. Chem.* **1992**, *96*, 4359−4366. Novoa, J. J.; Mota, F.; Alvarez, S. *J. Phys. Chem.* **1988**, *92*, 6561−6566. Gutsev, G. L. *Russ. J. Phys. Chem.* **1992**, *96*, 1596−1599. Cahill, P. A.; Dykstra, C. E.; Martin, J. C. *J. Am. Chem. Soc.* **1985**, *107*, 6359−6362.

(17) Landrum, G. A.; Goldberg, N.; Hoffmann, R. *J. Chem. Soc., Dalton Trans.* **1997**, 3605−3613. Munzarova, M. L.; Hoffmann, R. *J. Am. Chem. Soc.* **2002**, *124*, 4787−4795.

(18) See, for example: Silverberg, M. *Chemistry*, 2nd ed.; McGraw-Hill: Boston, 2000. Brady, J. E.; Russell, J. W.; Holum, J. R. *Chemistry: Matter and Its Changes*, 3rd ed.; Wiley: New York, 2000. McMurry, J.; Fay, R. C. *Chemistry*, 3rd ed.; Prentice Hall: Upper Saddle River, NJ, 2001. Chang, R. *Chemistry*, 7th ed.; McGraw-Hill: Boston, 2002. Ebbing, D. D.; Gammon, S. D. *General Chemistry*, 7th ed.; Houghton Mifflin: Boston, 2002. Moore, J. W.; Stanitski, C. L.; Jurs, P. C. *Chemistry: The Molecular Science*; Harcourt: Philadelphia, 2002. Jones, L. L.; Atkins, P. W. *Chemistry: Molecules, Matter and Change*, 4th ed.; W. H. Freeman: New York, 2000. Zumdahl, S. S.; Zumdahl, S. A. *Chemistry*, 5th ed.; Houghton Mifflin: Boston, 2000. Brown, T. L.; LeMay, H. E.; Bursten, B. E. *Chemistry: The Central Science*, 9th ed.; Prentice Hall: Upper Saddle River, NJ, 2003. The latter three books do mention alternative explanations for hypervalent bonding.

(19) Hach, R. J.; Rundle, R. E. *J. Am. Chem. Soc.* **1951**, *73*, 4321−4324.

(20) Pimentel, G. C. *J. Chem. Phys.* **1951**, *19*, 446−448.

(21) Kutzelnigg, W. *Angew. Chem., Int. Ed. Engl.* **1984**, *23*, 272−295.

(22) Kaupp, M.; van Wüllen, Ch.; Franke, R.; Schmitz, F.; Kutzelnigg, W. *J. Am. Chem. Soc.* **1996**, *118*, 11939−11950.

(23) Häser, M. *J. Am. Chem. Soc.* **1996**, *118*, 7311−7325. Cioslowski, J.; Mixon, S. T. *Inorg. Chem.* **1993**, *32*, 3209−3216.

(24) Noury, S.; Silvi, B.; Gillespie, R. J. *Inorg. Chem.* **2002**, *41*, 2164−2172.

(25) Pauling, L. *The Nature of the Chemical Bond*, 2nd ed.; Cornell University Press: Ithaca, NY, 1940.

(26) Nizzi, K. E.; Pommerening, C. A.; Sunderlin, L. S. *J. Phys. Chem. A* **1998**, *102*, 7674−7679.

(27) Moc, J.; Morokuma, K. *Inorg. Chem.* **1994**, *33*, 551−560.

(28) Bettinger, H. F.; Schleyer, P. v. R.; Schaefer, H. F., III. *J. Am. Chem. Soc.* **1998**, *120*, 11439−11448.

(29) Gutsev, G. L. *J. Chem. Phys.* **1993**, *98*, 444−452.

(30) Tschumper, G. S.; Fermann, J. T.; Schaefer, H. F., III. *J. Chem. Phys.* **1996**, *104*, 3676−3683.

(31) Gu, J.; Chen, K.; Xie, Y.; Schaefer, H. F., III.; Morris, R. A.; Viggiano, A. A. *J. Chem. Phys.* **1998**, *108*, 1050−1054.

(32) Gutsev, G. L. *Chem. Phys.* **1994**, *179*, 325−339.

(33) Muntean, F.; Armentrout, P. B. *J. Chem. Phys.* **2001**, *115*, 1213−1228 and references therein.

(34) Armentrout, P. B. *J. Am. Soc. Mass Spectrom.* **2002**, *13*, 419−434.

(35) Do, K.; Klein, T. P.; Pommerening, C. A.; Sunderlin, L. S. *J. Am. Soc. Mass Spectrom.* **1997**, *8*, 688−696.

(36) Ervin, K. M.; Armentrout, P. B. *J. Chem. Phys.* **1985**, *83*, 166−189. Rodgers, M. T.; Ervin, K. M.; Armentrout, P. B. *J. Chem. Phys.* **1997**, *106*, 4499−4508.

(37) Nakamoto, K. *Infrared and Raman Spectra of Inorganic and Coordination Compounds Part A: Theory and Applications in Inorganic Chemistry*, 5th ed.; John Wiley & Sons: New York, 1997.

(38) Lugez, C. L.; Irikura, K. K.; Jacox, M. E. *J. Chem. Phys.* **1998**, *108*, 8381−8393.

(39) Glukhovtsev, M. N.; Pross, A.; McGrath, M. P.; Radom, L. *J. Chem. Phys.* **1995**, *103*, 1878−1885.

(40) Check, C. E.; Faust, T. O.; Bailey, J. M.; Wright, B. J.; Gilbert, T. M.; Sunderlin, L. S. *J. Phys. Chem. A* **2001**, *105*, 8111−8116.

(41) Loh, S. K.; Hales, D. A.; Lian, L.; Armentrout, P. B. *J. Chem. Phys.* **1989**, *90*, 5466−5485. Schultz, R. H.; Crellin, K. C.; Armentrout, P. B. *J. Am. Chem. Soc.* **1991**, *113*, 8590−8601.

(42) Frisch, M. J.; Trucks, G. W.; Schlegel, H. B.; Scuseria, G. E.; Robb, M. A.; Cheeseman, J. R.; Zakrzewski, V. G.; Montgomery, J. A., Jr.; Stratmann, R. E.; Burant, J. C.; Dapprich, S.; Millam, J. M.; Daniels, A. D.; Kudin, K. N.; Strain, M. C.; Farkas, O.; Tomasi, J.; Barone, V.; Cossi, M.; Cammi, R.; Mennucci, B.; Pomelli, C.; Adamo, C.; Clifford, S.; Ochterski, J.; Petersson, G. A.; Ayala, P. Y.; Cui, Q.; Morokuma, K.; Malick, A D.; Rabuck, K. D.; Raghavachari, K.; Foresman, J. B.; Cioslowski, J.; Ortiz, J. V.; Baboul, A. G.; Stefanov, B. B.; Liu, G.; Liashenko, A.; Piskorz, P.; Komaromi, I.; Gomperts, R.; Martin, R. L.; Fox, D. J.; Keith, T.; Al-Laham, M. A.; Peng, C. Y.; Nanayakkara, A.; Challacombe, M.; Gill, P. M. W.; Johnson, B.; Chen, W.; Wong, M. W.; Andres, J. L.; Gonzalez, C.; Head-Gordon, M.; Replogle, E. S.; Pople. J. A. *Gaussian 98*, revision A.9; Gaussian, Inc.: Pittsburgh, PA, 1998.

(43) NBO 5.0.: Glendening, E. D.; Badenhoop, J. K.; Reed, A. E.; Carpenter, J. E.; Bohmann, J. A.; Morales, C. M.; Weinhold, F. Theoretical Chemistry Institute, University of Wisconsin, Madison, WI, 2001. http://www.chem.wisc.edu/~nbo5.

(44) Cioslowski, J.; Mixon, S. T. *Inorg. Chem.* **1993**, *32*, 3209−3216.

(45) Bader, R. F. W. *Atoms in Molecules: A Quantum Theory*; Clarendon Press: Oxford, U.K., 1990.

(46) Cioslowski, J.; Nanayakkara, A.; Challacombe, M. *Chem. Phys. Lett.* **1993**, *203*, 137−142. Cioslowski, J.; Surjan, P. R. *J. Mol. Struct.* **1992**, *255*, 9−33. Cioslowski, J.; Stefanov, B. B. *Mol. Phys.* **1995**, *84*, 707−716. Stefanov, B. B.; Cioslowski, J. R. *J. Comput. Chem.* **1995**, *16*, 1394−1404. Cioslowski, J. *Int. J. Quantum Chem. Quantum Chem. Symp.* **1990**, *24*, 15−28. Cioslowski, J.; Mixon, S. T. *J. Am. Chem. Soc.* **1991**, *113*, 4142. Cioslowski, J. *Chem. Phys. Lett.* **1992**, *194*, 73−78. Cioslowski, J. *Chem. Phys. Lett.* **1994**, *219*, 151−154.

(47) Wells, A. F. *Structural Inorganic Chemistry*, 5th ed.; Clarendon Press: Oxford, U.K., 1984.

(48) Cotton, F. A.; Wilkinson, G.; Murillo, C. A.; Bochmann, M. *Advanced Inorganic Chemistry*, 6th ed.; Wiley-Interscience: New York, 1999.

(49) Reference 48, p 395.

(50) Mingos, D. M. P. *Essential Trends in Inorganic Chemistry*; Oxford University Press: Oxford, NY, 1998.

(51) Chase, M. W., Jr. *NIST-JANAF Thermochemical Tables*, 4th ed.; National Institute of Standards and Technology: Gaithersburg, MD, 1998. (*J. Phys. Chem. Ref. Data*, Monograph 9.) Solid-state heat of formation and estimated heat of vaporization for PI_3 taken from data in ref 1.

(52) Gailbreath, B. D.; Pommerening, C. A.; Bachrach, S. M.; Sunderlin, L. S. *J. Phys. Chem, A* **2000**, *104*, 2958−2961. Bachrach, S. M.; Hayes, J. M.; Check, C. E.; Sunderlin, L. S. *J. Phys. Chem. A* **2001**, *105*, 9595−9597.

(53) Hiraoka, K.; Shimizu, A.; Minamitsu, A.; Nasu, M.; Fujimaki, S.; Yamabe, S. *Chem. Phys. Lett.* **1995**, *241*, 623−626.

(54) Artau, A.; Nizzi, K. E.; Hill, B. T.; Sunderlin, L. S.; Wenthold, P. G. *J. Am. Chem Soc.* **2000**, *122*, 10667−10670.

(55) Shurki, A.; Hiberty, P. C.; Shaik, S. *J. Am. Chem. Soc.* **1999**, *121*, 822−834.

(56) Sini, G.; Ohanessian, G.; Hiberty, P. C.; Shaik, S. *J. Am. Chem. Soc.* **1990**, *112*, 1407−1413.